ISSN: 2472-3703 DOI: 10.6911/WSRJ.202208_8(8).0054

Fe/N co-doped Biocarbon Materials and Their Catalytic Oxidative Degradation of Antibiotic Wastewater

Chaoting Fu[1], Bo Xing[1, 2, *], Siyang Zhang[1], Yuling Ye[1], Guo Yang[1, 2, *], Xingyong Liu[1, 2], Zhongcai Pan[1], Junjie You[1], Qian Zhou[1], Ziyu Wang[1]

[1]School of Chemical Engineering, Sichuan University of Science and Engineering, Zigong 643000, PR China

[2]National Engineering Research Center for Municipal Wastewater Treatment and Reuse, Mianyang 621000, PR China

Abstract

The removal effect of Fe/N co-doped biocarbon materials (Fe/N-ACs) in catalytic persulfate-catalyzed degradation of tetracycline hydrochloride (TC) was studied in order to seek a catalyst with high catalytic activity in antibiotic wastewater treatment. Using melamine and ferric nitrate as nitrogen source and iron source, respectively, and using distiller's grains as carbon source, the Fe/N-ACs catalysts with different nitrogen content ratios and different calcination temperatures were prepared by the method of blending grinding and carbon dioxide activation. Then it was used to analyze its removal effect on TC. Activated carbon (AC) prepared from distiller's grains alone catalyzed the decomposition of 25.0% of TC, which was proportional to the removal of TC with the increase of nitrogen content and calcination temperature. When the Fe content is 5%, the melamine content is 20%, and the calcination temperature is 850 °C, the catalyst has good catalytic performance. Under optimal conditions, after 1h of reaction, the removal rate of TC can reach 61.1%. Fe/N-ACs have a synergistic effect on catalyzing persulfate.

Keywords

Persulfate; Fe/N modification; Antibiotic wastewater; Biomass.

1. INTRODUCTION

In recent years, pollution in water bodies has attracted widespread public attention. Most harmful and toxic pollutants, including antibiotics, dyes, pesticides, etc., threaten human health. Among the many methods for treating organic wastewater, sulfate ($SO_4^{\bullet-}$)-based advanced oxidation processes (SR-AOPs) have received increasing attention in wastewater treatment. Because the advanced oxidation technology based on $SO_4^{\bullet-}$ has a high redox potential (2.5-3.1V) compared with the hydroxyl radical (•OH) generated by the traditional Fenton oxidation, is not dependent on pH, and has a long reaction life [1]. $SO_4^{\bullet-}$ can be generated by ultraviolet [2], heating [3], microwave [4] and transition elements (Fe, Ag, Co, etc.) [5-7] activated peroxymonosulfate (PMS) or persulfate (PS). However, heating, UV and microwave means consume a lot of energy. The dissolution of metal ions may lead to secondary pollution.

Carbon material supports have the advantages of large specific surface area, high chemical stability, and good electrical conductivity. Therefore, it can be used to support metals and effectively reduce the dissolution of metal ions. Biochar can be produced from biomass waste with low cost and abundant sources. Dispersing metal oxides on biochar substrates can improve material stability and catalytic activity [8].

ISSN: 2472-3703 DOI: 10.6911/WSRJ.202208_8(8).0054

Unmodified carbon-based materials can activate PS to remove organic pollutants, but the ability to activate PS is limited. In order to improve its catalytic activity, heteroatom doping can be used. Common heteroatoms include N, P, and S, which is a simple and effective method to enhance biomass activated carbon [9]. The use of N atom doping to replace carbon atoms in carbon materials is considered to be one of the optimal modification methods. Wang[10] showed that nitrogen-doped modified BCs (NBCs) enhanced the performance of catalytic PS and sulfadiazine degradation ability compared with pristine BCs. Iron and iron oxide nanoparticles have been shown to effectively activate PMS [11]. Iron-nitrogen co-doping has been reported to significantly enhance the ability of catalytically activated PS [12]. Since the nitrogen-doped in the carbon framework contains a large number of lone pairs of electrons, it can act as a Lewis base site. The iron sites act as Lewis acid sites and are effectively anchored in the carbon-nitrogen matrix to form new Fe-Nx active sites. The newly generated active sites can often induce significant catalytic effects due to their unique electronic structures and close interactions with supports [13].

Therefore, in this paper, Fe/N co-doped biochar (Fe/N-ACs) was prepared by using distiller's grains as carbon source, melamine as N source and $Fe(NO_3)_3$ as iron source. The effect of preparation process (nitrogen content and calcination temperature) on the removal of tetracycline hydrochloride by activated PS was studied. The main reactive oxygen species (ROS) in Fe/N-ACs activated PS system were investigated by free radical quenching test. We believe that this study provides a new way for the utilization of distiller's grains.

2. MATERIALS AND METHODS

2.1. Chemicals and Materials

Sodium persulfate (PS), melamine, $Fe(NO_3)_3$, methanol (MeOH), tert-butanol (TBA), methylene blue (MB), rhodamine B (Rh B), and methyl orange (MO) were purchased from Kelong Chemical Reagent Co., Ltd. (Chengdu, China). Acid red 73(AR 73) and tetracycline hydrochloride (TC) were purchased from Aladdin Co., Ltd. (Shanghai, China). All chemicals are analytical grade reagents. distiller's grains were purchased from Wuliangye Yibin Co., Ltd. (Yibin, China). The UV-visible spectrophotometer (UV-1100) was purchased from Shanghai Meipuda Instrument Co., Ltd.

2.2. Material Preparation

First, the raw distiller's grains were pulverized and ground with melamine and ferric nitrate in different proportions, and then put into a tubular heating furnace, and calcined at a constant temperature of 650-850 °C for 1 h under N_2 atmosphere to obtain carbonized samples. Secondly, the carbonized samples were acid-washed with HCl solution for 12 h, washed with deionized water until the pH did not change, and dried to obtain the acid-washed carbonized samples. Finally, the carbonized samples after pickling were put into a tube furnace and activated at a constant temperature of 800 °C for 2 h in a CO_2 atmosphere to obtain Fe/N-ACs. The catalyst obtained here is labeled aFe-bN-AC-T. Wherein a represents the mass percentage of m (ferric nitrate)/(distillers grains), b represents the mass percentage of m (melamine)/(distillers grains), T represents the carbonization temperature, °C. For example, the catalyst numbered 5Fe-20N-AC-750 indicates that the mass percentage of m (iron nitrate)/(distillers grains) is 5%, the mass percentage of m (melamine)/(distillers grains) is 20%, and the carbonization temperature is 750 °C .

2.3. Characterizations

The N_2 adsorption/desorption isotherms were measured by a 3H-200PM2 instrument of Best Instrument Technology (Beijing) Co., Ltd. The total pore volume (V_t) is the volume of N_2

ISSN: 2472-3703 DOI: 10.6911/WSRJ.202208_8(8).0054

adsorbed at a P/P_0 of 0.995. The specific surface area (S_{BET}) was calculated according to the BET equation. Mesopore pore size distribution and mesopore volume (V_{meso}) were calculated according to the BJH model. Diffraction analysis of activated carbon was carried out using a Bruker/D2 PHASER ray diffractometer from Bruker AXE Company, Germany. The H_2-TPD was tested on an AutoChem II Model 2920 from Mack. Raman scattering spectra were collected using a LabRAM HR800 (Horiba Jobin Yvon, FR.) spectrometer.

2.4. Catalytic Persulfate Degradation of TC

The removal rate of tetracycline hydrochloride was used as the basis for evaluating the catalytic performance. The experimental steps are as follows: take 250 mL of tetracycline hydrochloride solution with a concentration of 20 mg/L in a three-necked flask, and adjust the pH with 0.1 mol/L HCl solution or 0.1 mol/L NaOH solution. Then, after rising to the specified temperature, the oxidant PS and Fe/N-ACs catalyst were added and stirred magnetically. Finally, samples were taken at regular intervals, and the absorbance of tetracycline hydrochloride was measured by a spectrophotometer at $\lambda = 356$ nm. Through standard curve conversion, the actual concentration can be obtained.

3. RESULTS AND DISCUSSION

3.1. N_2 adsorption/Desorption Isotherms

A series of Fe/N-ACs were obtained with different amounts of nitrogen-containing precursors and calcination temperatures, and their N_2 isothermal adsorption/desorption curves are shown in Figure 1, and their structural parameters are shown in Table 1.

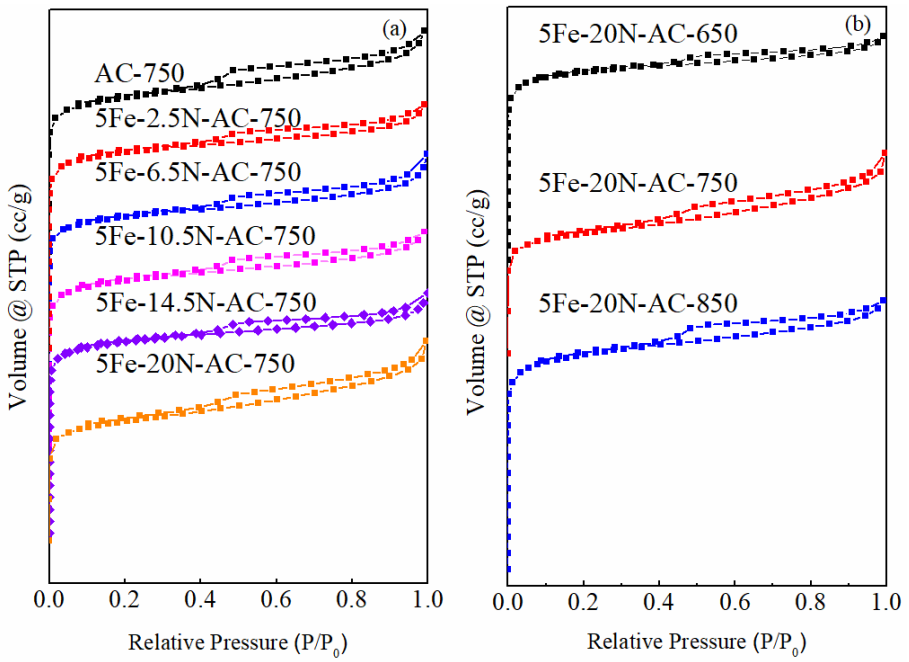

Figure 1. N_2 adsorption/desorption isotherms of Fe/N-ACs with different nitrogen content (a) and calcination temperature (b)

ISSN: 2472-3703 DOI: 10.6911/WSRJ.202208_8(8).0054

Table 1. Structural parameters of porous carbon materials with different amounts of nitrogen-containing precursors and calcination temperatures

Catalyst	SBET (m^2/g)	Vt (cm^3/g)	Vmeso (cm^3/g)	Vmeso/Vt	D&BJH-average (nm)	D*BJH (nm)
AC-750	238.52	0.164	0.116	0.707	4.7	3.8
5Fe-2.5N-AC-750	267.85	0.167	0.134	0.802	4.5	3.8
5Fe-6.5N-AC-750	248.53	0.169	0.123	0.728	5.1	3.8
5Fe-10.5N-AC-750	266.95	0.167	0.133	0.796	4.3	3.8
5Fe-14.5N-AC-750	295.41	0.182	0.145	0.797	4.4	3.8
5Fe-20N-AC-750	299.66	0.225	0.146	0.649	5.2	3.9
5Fe-20N-AC-650	324.15	0.193	0.161	0.834	4.1	3.8
5Fe-20N-AC-850	272.35	0.170	0.135	0.794	4.1	3.8

Note: & represents the average pore size, * represents the most probable pore size

According to the classification of IUPAC adsorption isotherms, it can be seen from Figure 1(a) and (b) that the isotherms of the catalysts belong to type IV [1]. And different nitrogen content and calcination temperature did not have a significant effect on the hysteresis loop. It can be seen from Table 1 that the obtained series of Fe/N-ACs is a porous carbon material mainly composed of mesopores, the mesopore volume can reach more than 0.123 cm^3/g, and the average pore diameter is 4.1 nm. It shows that the prepared carbon material is mainly composed of mesopores. Corresponding to the above analysis, the specific surface area, pore diameter, pore volume and other data of all samples are shown in Table 1. With the increase of the amount of N source, the specific surface area and pore size of carbon materials also tend to increase. 5Fe-20N-AC-750 has the largest specific surface area, pore diameter and total pore volume, which are 299.66 m^2/g, 3.9 nm and 0.23 cm^3/g, respectively. This is due to the modification of the surface of carbon materials by N element, because N element has excellent performance in the opening and expansion of carbon materials. Therefore, compared with 5Fe-20N-AC-750, the specific surface area, pore diameter and pore volume of 5Fe-2.5N-AC-750 were reduced to 267.85 m^2/g, 3.8 nm, and 0.17 cm^3/g, respectively. For different calcination temperatures, the specific surface area showed a decreasing trend, possibly due to the partial collapse of the pore structure due to high temperature.

3.2. XRD Analysis

It can be seen from Figure 2(a) that the spectra of the prepared six porous carbon materials are basically the same, and there are obvious diffraction peaks at 26.6°. 26.6° corresponds to the (002) plane of the graphite crystal [14]. The characteristic peaks of Fe3O4 appear at $2\theta=35.3°$ and 62.6°, but the peak intensity is not obvious, indicating that the content is less [15]. The diffraction peaks displayed in the XRD patterns are all broad and diffuse peaks, which proves that all the materials are amorphous carbons. In Figure 2(b), the XRD patterns at different calcination temperatures show similar morphology, indicating that high temperature has no obvious effect on its crystal structure.

ISSN: 2472-3703 DOI: 10.6911/WSRJ.202208_8(8).0054

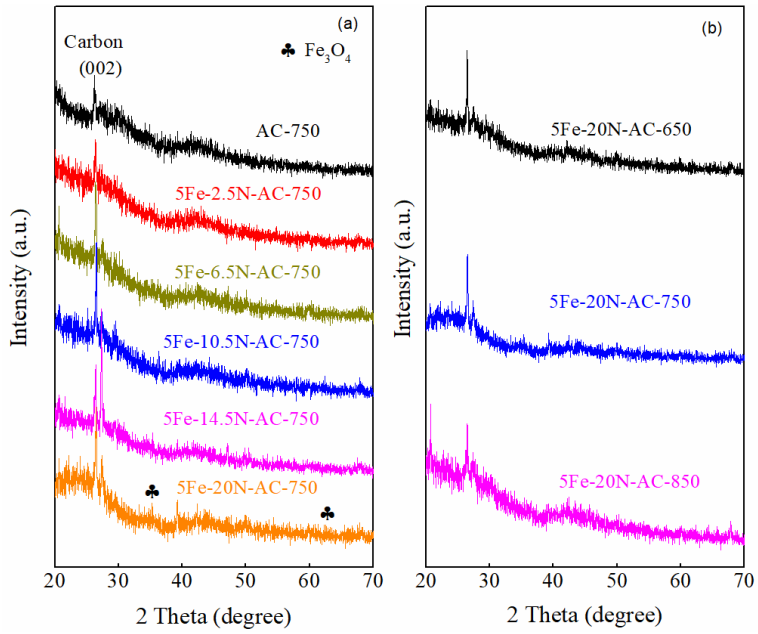

Figure 2. XRD spectra of Fe/N-ACs with different nitrogen content (a) and calcination temperature (b)

3.3. H_2-TPR Analysis

H_2-TPR characterization can reflect the redox performance of the prepared samples under the reducing atmosphere of supported metal catalysts. In Figure 3(a), the effects of different nitrogen contents on the reduction temperature were investigated by controlling the addition of $Fe(NO_3)_3$ in the same proportion. It can be seen that there is no reduction peak for AC-750 alone. This is because AC is calcined at high temperature, and even if the surface contains oxygen-containing functional groups, it will decompose. The H_2-TPR peaks are concentrated at 410 ~ 440°C, which may be related to the reduction of Fe^{3+} to Fe^{2+} and the reduction of Fe_2O_3 oxides to Fe_3O_4. This is consistent with the result of Fe_3O_4 detected by XRD. With the increase of nitrogen content, the reduction peak shifted to low temperature, indicating that the presence of nitrogen is beneficial to the reduction of Fe_2O_3. When the nitrogen content is 6.5%, the temperature of the reduction peak is the highest. It may be that during the grinding process, the dispersion of N is more uniform, making it easier for Fe species to enter the interior of the material framework and then form complexes with N. Therefore restoration is more difficult [16].

Figure 3(b) shows the effect of different calcination temperatures on the reduction temperature. It can be seen that when the calcination temperature is increased, the low temperature peak (about 402 °C) gradually rises. According to previous reports, the reduction behavior of iron oxides is affected by morphology, particle size, crystallinity, and defect density. When the low temperature peak shifts to the high temperature peak, larger grains are formed, which makes it difficult to reduce [17].

ISSN: 2472-3703 DOI: 10.6911/WSRJ.202208_8(8).0054

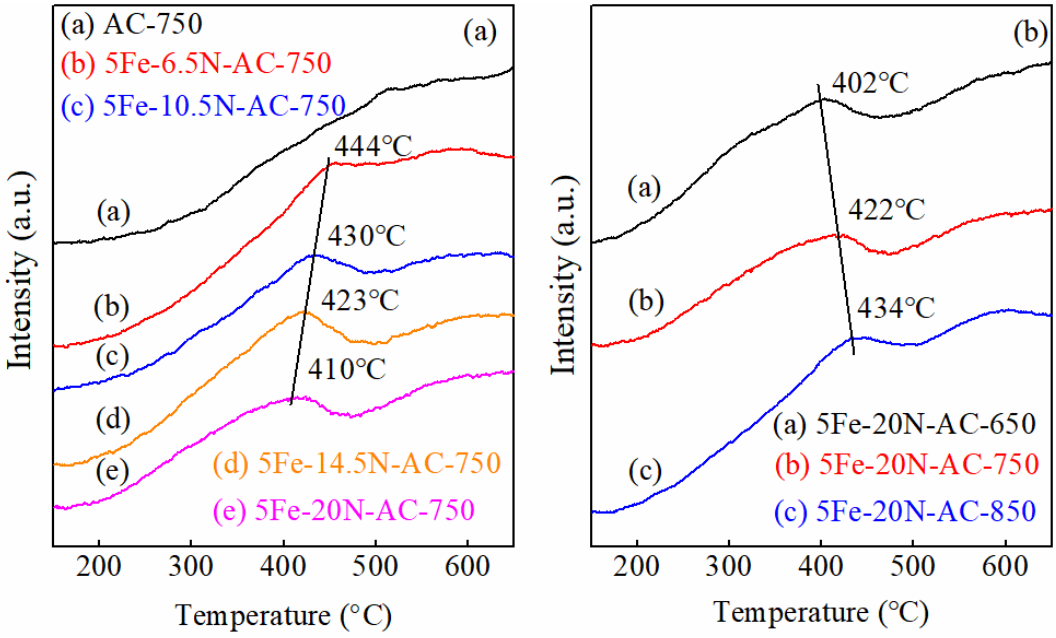

Figure 3. H_2-TPR of Fe/N-ACs with different nitrogen content (a) and calcination temperature (b)

3.4. Raman Analysis

It can be seen from Figure 4 that there are obvious D-bands (1335 cm^{-1}) and G-bands (1588 cm^{-1}) under different carbonization temperatures. The D band represents the lattice defects of carbon atoms, and the G band represents the in-plane stretching vibration of the sp^2 orbital hybridization of carbon atoms. The peak intensity and peak width of the D band largely depend on the structural properties of the functional groups of disordered carbons and their uniformity. There is a strong D-band and a weaker G-band. The intensity ratio of D band to G band (I_D/I_G) represents the degree of graphitization of the catalyst [1]. It can be seen from Figure 4 that the I_D/I_G values of Fe/N-ACs at different carbonization temperatures are 1.84, 1.53, and 1.51, respectively. Among the prepared catalysts, the catalyst prepared at a carbonization temperature of 850 °C had the smallest value of I_D/I_G and the highest degree of graphitization. It can be seen that with the gradual increase of carbonization temperature, it is beneficial to improve the degree of graphitization of the catalyst.

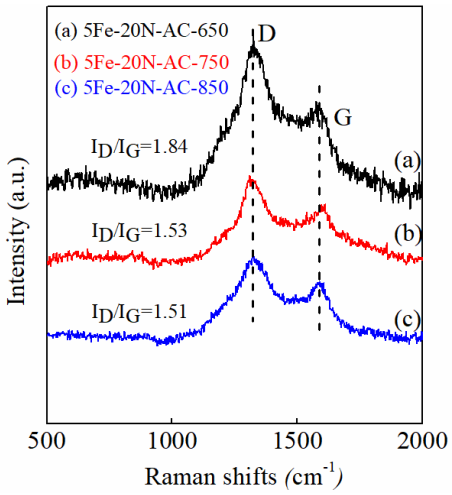

Figure 4. Raman spectrum

ISSN: 2472-3703 DOI: 10.6911/WSRJ.202208_8(8).0054

3.5. Catalytic Degradation of TC by Fe/N-ACs with Different Nitrogen Contents

The results of the catalytic degradation of TC by Fe/N-ACs with different nitrogen contents are shown in Figure 5(a). When PS was used alone, the removal rate of TC was only 5.1%. The use of unmodified AC has a certain effect on the activation of PS, and the removal rate reaches 25.0%. When Fe and N were loaded on the catalyst, and with the increase of the amount of nitrogen-containing precursor in the catalyst, the removal rate was positively correlated. As shown in Figure 5(b), the reaction rate constant (k_{app}) number is up to 0.009 min^{-1}, which is 1.94 times higher than that of unmodified AC. Comparing the adsorption capacity of catalyst 5Fe-20N-AC-750, it can only adsorb 2.5% TC at 60 min. It can be seen that the local electronic structure of the porous carbon material surface is regulated by Fe/N co-doping. N element enhances the catalytic activation performance and adsorption performance of porous carbon materials, and improves the stability of the supported metal, while the loading of metallic iron increases the interaction with N element. When the amount of nitrogen-containing precursor was 20%, the removal rate reached 43.1%.

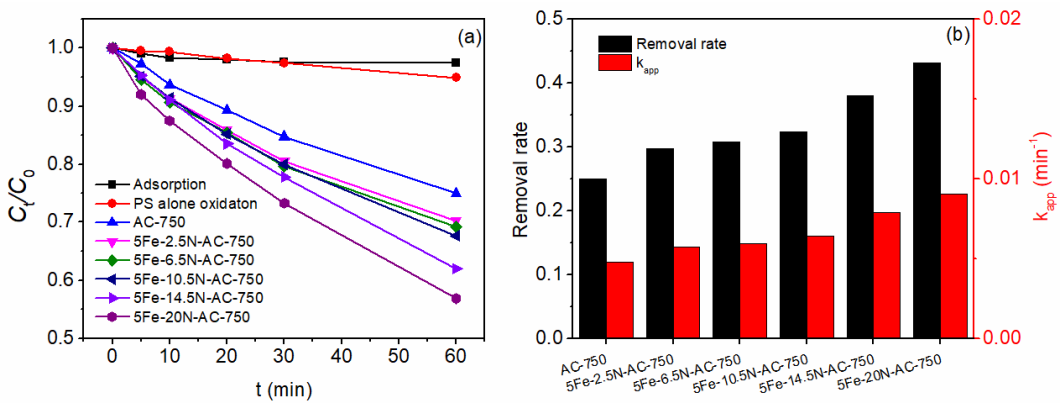

Figure 5. The effect of porous carbon with different nitrogen contents on TC degradation (a) and the removal rate and reaction rate of TC under porous carbon with different nitrogen contents (b) (Reaction conditions: C_0=20 mg/L, T=30 °C, PS=1.2 g/L, Cat=0.2 g/L, pH=6)

3.6. Effects of Different Calcination Temperatures on Catalytic PS Degradation of TC

It can be seen from Figure 6(a) that the removal rate of TC gradually increased with the increase of carbonization temperature when the reaction was carried out for 60 min. When the carbonization temperature was 650 °C~850 °C, the removal rates were 42.1%, 43.1%, and 48.4%. The k_{app} of catalysts with different calcination temperatures increased from 0.009 to 0.011 min^{-1}. Combined with the results of specific surface area, it can be seen that the specific surface area of 5Fe-20N-AC-850 is the smallest, but the catalytic effect is the best. This may be due to the fact that with the increase of carbonization temperature, the pyrolysis degree of distiller's grains deepens and the degree of graphitization gradually increases, resulting in a gradual increase in catalytic activity. It shows that the degree of graphitization is the key factor affecting its activity.

ISSN: 2472-3703 DOI: 10.6911/WSRJ.202208_8(8).0054

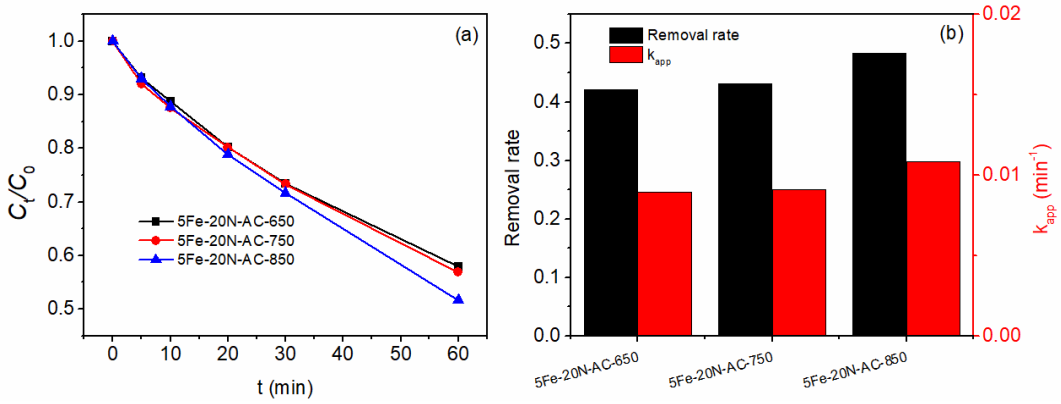

Figure 6. The effect of Fe/N-ACs at different calcination temperatures on TC degradation (a) and the removal rate and reaction rate of TC under Fe/N-ACs conditions with different calcination temperatures (b) (Reaction conditions: C_0=20 mg/L, T=30 °C, PS=1.2 g/L, Cat=0.2 g/L, pH=6)

3.7. Quenching Experiments

To explore the active species in catalytic reactions. Tert-butanol and methanol were used as quenchers. MeOH is usually used to quench HO· and $SO_4^{\bullet-}$ in catalytic reactions. The reaction rates of MeOH with HO· and $SO_4^{\bullet-}$ are $k_{HO\cdot}$=(0.83-1) ×10^9 $M^{-1}s^{-1}$ and $k_{SO4\bullet-}$=1×10^7 $M^{-1}s^{-1}$. TBA only has a good quenching effect on HO·, because its reaction rate is about 1000 times that of $SO_4^{\bullet-}$[1]. As shown in Figure 7, after the HO· masking experiment was carried out with the addition of TBA, the removal rate decreased from 62.77% to 28.86%, a decrease of 45.9%, and the addition of the quencher had a great influence on the removal rate. After adding methanol to carry out the $SO_4^{\bullet-}$ masking experiment, the removal rate decreased from 62.77% to 31.31%, a decrease of 49.9%. The addition of quencher also had a great influence on the removal rate. Combined with the results obtained in the previous adsorption test of the catalyst, the removal rate was only 2.5%, and the adsorption performance of the prepared catalyst was not strong, so it was speculated that the reaction occurred in solution. The active site on the catalyst promotes the oxidant to decompose more free radicals, so the effect of the addition of a quencher on the experimental results is so obvious.

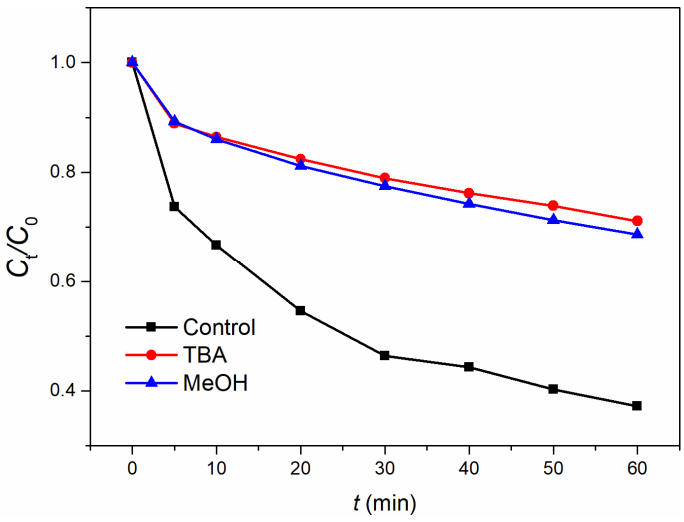

Figure 7. Influence of different scavengers on TC degradation (Reaction conditions: C_0=20 mg/L, T=35 °C, PS=1.6 g/L, Cat=0.4 g/L, pH=3)

ISSN: 2472-3703 DOI: 10.6911/WSRJ.202208_8(8).0054

3.8. Degradation of Different Organic Pollutants

In order to broaden the application range of the catalyst, several common organic pollutants were selected for experiments under optimal conditions. It can be seen from Figure 8 that the removal rates of Rh B, MB, AR 73 and MO were 76.5%, 73.2%, 95.6% and 89.1%, respectively, after 60 min of reaction. It can be seen from the above results that under the same conditions, the effect of degrading the dye is higher than that of TC. So it can also be applied to other pollutants.

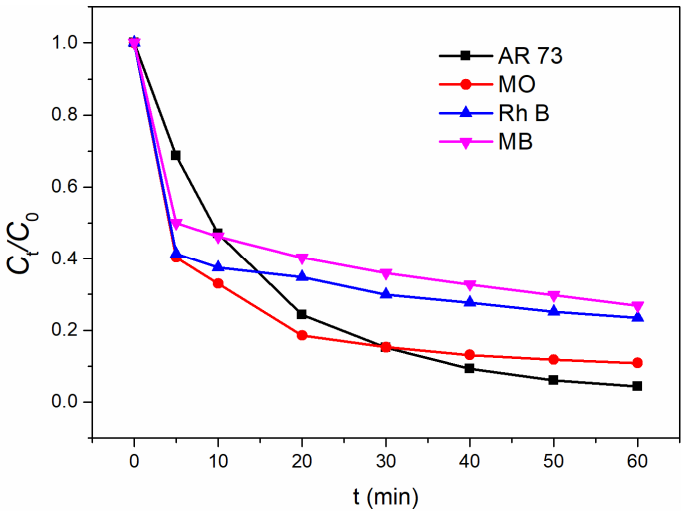

Figure 8. Degradation effect of different organic pollutants (Reaction conditions: C_0=20 mg/L, T=35 °C, PS=1.6 g/L, Cat=0.4 g/L, pH=3)

3.9. CatalyticStability and Reusability of 5Fe-20N-AC-850

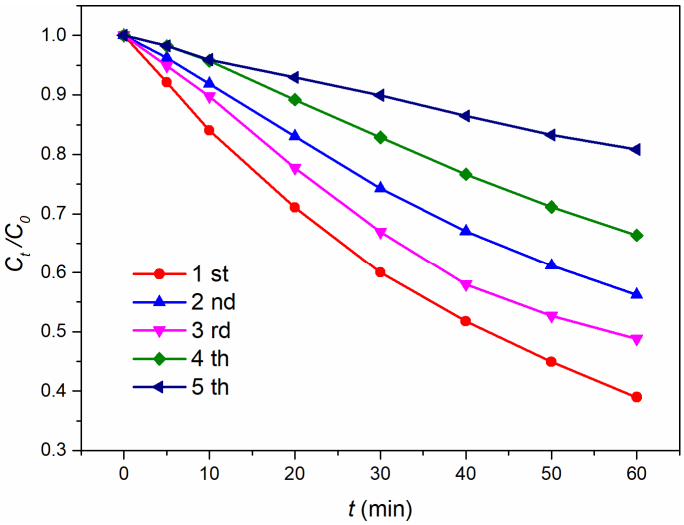

Figure 9. Catalyst cycle times (Reaction conditions: C_0=20 mg/L, T=35 °C, PS=1.6 g/L, Cat=0.4 g/L, pH=3)

It can be seen from Figure 9 that after the reaction for 60 min, the removal rate after the first reuse is 61.1%, the removal rate after the second reuse is 43.8%, and the removal rate after the third reuse is 51.2%. The removal rate of the third time was higher than that of the second time, which may be due to the escape of organic molecules on the active sites that were originally covered on the surface of the catalyst during the degradation process, and the activity of the catalyst was recovered to a certain extent. As a result, the number of reuses increases and the

ISSN: 2472-3703 DOI: 10.6911/WSRJ.202208_8(8).0054

removal rate increases instead. After the catalyst was reused five times, the removal rate was 19.2%, which was a significant decrease compared to the first reuse. The final results show that the catalyst prepared in this study has a certain reusability, but the stability of the catalyst itself is not strong. The reason may be that during the experiment, tetracycline hydrochloride molecules entered the pores of the catalyst, covering the active sites on the surface of the catalyst, resulting in the deactivation of the catalyst.

4. CONCLUSION

(1) Fe/N-ACs were successfully prepared by one-step blending + CO_2 activation, in which nitrogen content and calcination temperature were beneficial to the improvement of catalytic activity, which was related to the degree of graphitization of porous carbon.

(2) The optimum process conditions are that the addition amount of PS is 1.6 g/L; the addition amount of 5Fe-20N-AC-850 is 0.4 g/L; T = 35 °C; pH = 3. The removal rate can reach 66.1% at 60 min.

(3) Radical masking experiments show that the catalytic degradation of TC is mainly due to the joint action of HO·and $SO_4^{\bullet-}$.

ACKNOWLEDGMENTS

This work is supported by the National Natural Science Foundation of China (22106112), Talents Introduction Program of Sichuan University of Science and Engineering (2020RC03), Returned Overseas Program of Sichuan University of Science and Engineering (2021RC25), Vanadium and Titanium Resources Utilization Key Laboratory of Sichuan Province (2018FTSZ12, 2018FTSZ18), Process Equipment and Control Engineering Key Laboratory of Sichuan Province (GK202008), Opening Project of Chemical Synthesis and Pollution Control Key Laboratory of Sichuan Province (CSPC202107), The Key Laboratory of Fine Chemical Application Technology of Luzhou (HYJH-2017-B), Zigong Provincial Transfer Payment Technology Support Program (2021SZYZF01).

REFERENCES

[1] M.F. Xi, K.P. Cui, M.S. Cui, et al. Enhanced norfloxacin degradation by iron and nitrogen co-doped biochar: Revealing the radical and nonradical co-dominant mechanism of persulfate activation [J]. Chem Eng J, Vol. 420 (2021) p. 129902.

[2] L. Cai, L. Li, S. Yu, et al. Formation of odorous by-products during chlorination of major amino acids in East Taihu Lake: Impacts of UV, UV/PS and UV/H2O2 pre-treatments [J]. Water Research, Vol. 162 (2019) p. 427-436.

[3] J. Wang, S. Wang. Activation of persulfate (PS) and peroxymonosulfate (PMS) and application for the degradation of emerging contaminants [J]. Chem Eng J, Vol. 334 (2018) p. 1502-1517.

[4] J. Guo, L. Zhu, N. Sun, et al. Degradation of nitrobenzene by sodium persulfate activated with zero-valent zinc in the presence of low frequency ultrasound [J]. Journal of the Taiwan Institute of Chemical Engineers, Vol. 78 (2017) p. 137-143.

[5] Q. Ji, J. Li, Z. Xiong, et al. Enhanced reactivity of microscale Fe/Cu bimetallic particles (mFe/Cu) with persulfate (PS) for p-nitrophenol (PNP) removal in aqueous solution [J]. Chemosphere, Vol. 172 (2017) p. 10-20.

[6] Y. Zhang, B.-T. Zhang, Y. Teng, et al. Activation of persulfate by core-shell structured Fe3O4@C/CDs-Ag nanocomposite for the efficient degradation of penicillin [J]. Separation and Purification Technology, Vol. 254 (2021) p. 117617.

ISSN: 2472-3703 DOI: 10.6911/WSRJ.202208_8(8).0054

[7] B. Li, Y.-F. Wang, L. Zhang, et al. Enhancement strategies for efficient activation of persulfate by heterogeneous cobalt-containing catalysts: A review [J]. Chemosphere, Vol. 291 (2022) p. 132954.

[8] J. Wang, S. Wang. Preparation, modification and environmental application of biochar: A review [J]. Journal of Cleaner Production, Vol. 227 (2019) p. 1002-1022.

[9] H. Wang, Y. Shao, S. Mei, et al. Polymer-Derived Heteroatom-Doped Porous Carbon Materials [J]. Chemical Reviews, Vol. 120 (2020) No.17, p. 9363-9419.

[10] H. Wang, W. Guo, B. Liu, et al. Edge-nitrogenated biochar for efficient peroxydisulfate activation: An electron transfer mechanism [J]. Water Research, Vol. 160 (2019) p. 405-414.

[11] S. Wang, Y. Liu, J. Wang. Iron and sulfur co-doped graphite carbon nitride (FeOy/S-g-C3N4) for activating peroxymonosulfate to enhance sulfamethoxazole degradation [J]. Chem Eng J, Vol. 382 (2020) p. 122836.

[12] X. Li, Y. Jia, M. Zhou, et al. High-efficiency degradation of organic pollutants with Fe, N co-doped biochar catalysts via persulfate activation [J]. Journal of Hazardous Materials, Vol. 397 (2020) p. 122764.

[13] J.-F. Sun, Q.-Q. Xu, J.-L. Qi, et al. Isolated Single Atoms Anchored on N-Doped Carbon Materials as a Highly Efficient Catalyst for Electrochemical and Organic Reactions [J]. Acs Sustainable Chemistry & Engineering, Vol. 8 (2020) No.39, p. 14630-14656.

[14] W. Miao, Y. Liu, D. Wang, et al. The role of Fe-Nx single-atom catalytic sites in peroxymonosulfate activation: Formation of surface-activated complex and non-radical pathways [J]. Chem Eng J, Vol. 423 (2021) p. 130250.

[15] Z. Peng, Z. Jianhua, P. Xiaoming, et al. Removal of tetracycline from water by activation of persulfate with Fe, N co-doped mesoporous materials [J]. Journal of Chemical Engineering of Chinese Universities, Vol. 35 (2021) No.06, p. 1090-1098. (In Chinese)

[16] B. Liu, H. Zhao, J. Yang, et al. Fe-containing N-doped porous carbon for isobutane dehydrogenation [J]. Microporous and Mesoporous Materials, Vol. 293 (2020) p. 109820.

[17] H. Zhou, K. Li, B. Zhao, et al. Surface properties and reactivity of Fe/Al2O3/cordierite catalysts for NO reduction by C2H6: Effects of calcination temperature [J]. Chem Eng J, Vol. 326 (2017) p. 737-744.